Tunable pulse advancement and delay by frequency-chirped stimulated Raman gain with optical nanofiber

YUN QI,[1,2] WEI JIN,[1,2,*] HOI LUT HO[1,2]

[1]*Department of Electrical Engineering, The Hong Kong Polytechnic University, Hong Kong, China*

[2]*Photonics Research Center, The Hong Kong Polytechnic University Shenzhen Research Institute, Shenzhen, China*

**Corresponding author: eewjin@polyu.edu.hk*

Received XX Month XXXX; revised XX Month, XXXX; accepted XX Month XXXX; posted XX Month XXXX (Doc. ID XXXXX); published XX Month XXXX

We demonstrate a novel method to optically tuning the pulse advancement and delay based on stimulated Raman gain in hydrogen. With a frequency chirped pump, the generated signal pulse is selectively amplified at the leading or trailing edge of the pump pulse, depending on whether the frequency difference between the pump and the signal beam is blue or red detuned from the Raman transition, which results in advancement or delay of the signal peak. Different from the method of slow/fast light, where advancement and delay are accompanied with power loss and gain respectively for a single resonance, both the advancement and delay are realized in the gain region for the method here. With a piece of 48-mm-long optical nanofiber in hydrogen, the time-shift for signal peak ranging from 3.7 to -3.7 ns is achieved in a Raman-generated pulse with width of ~12 ns.

All-optical control of the pulse delay is a building block for future optical network, where data buffering, synchronization and switching are expected to be based on all-optical devices with potentially much higher speed than the electronic counterparts [1]. The vast majority of implementations of pulse delay control are based on slow/fast light technique, where group velocity of the signal pulse is made significantly different from the normal condition [2]. Generally, the signal beam should locate at the vicinity of a gain/loss spectral resonance, where the refractive index is modified according to the Kramers-Kronig relations. The induced dispersion then results in change of group velocity and thus time of arrival for the signal. In the atomic system, marvelous results of slow/fast light based on electromagnetically induced transparency (EIT) [3], double-resonance [4] and coherent population oscillation (CPO) [5] have been achieved. However, the operation band of the systems are limited due to the available transition lines. Stimulated Brillouin scattering (SBS) [6-9] and stimulated Raman scattering (SRS) [10, 11] in optical fibers and silicon chips have also been exploited for controlling the group velocity of pulses, with high flexibility in operating wavelength and inherent compatibility with optical fiber communication systems. Besides the slow/fast light technique, dispersive delay line (DDL) is another popular method developed [12]. It is a combination of wavelength conversion in a nonlinear medium and group velocity dispersion in a highly dispersive fiber. Delays as large as thousands of pulse width can be achieved with kilometers long dispersive fiber. However, for all the techniques discussed above, although the magnitude of delay can be optically controlled, the sign of delay may not be easily changed, i.e., the systems are basically designed for either pulse advancement or delay. An elaborate method of reconfigurable gain profile base on SBS is reported to be able to operate in both the advancement and delay modes, but the system is complex and the switching is not straightforward [13].

Here, we report a totally different method which is based on the stimulated Raman gain (SRG) in gas-phase medium with a frequency chirped pump pulse. The arrival of signal peak can be readily switched between advancement and delay with slight tuning of the optical frequency across the gain profile of Raman transition. The technique is verified by experiments conducted on the optical nanofiber (NF) platform with pure hydrogen as the gain medium in its evanescent field. A tunable delay for the signal peak ranging from -3.7 to 3.7 ns is achieved with frequency-chirped pump pulse induced by self-phase-modulation (SPM). It is observed that the signal peak can have already exited the nanofiber before the pump peak entering into it.

In SRG process, the signal beam is amplified by the pump beam with gain proportional to pump intensity. The gain is the largest when the frequency difference between the pump and signal matches with the Raman resonance at υ_R. For a temporally Gaussian-shaped pump pulse, the signal gain is the largest at the pulse center, where the intensity is the highest. However, if the pump pulse is frequency chirped with a chirping amplitude comparable to the linewidth of the gain profile, the situation will be different. Suppose a continuous wave (cw) signal beam with fixed frequency of ν_s is Raman-amplified by a Gaussian-shaped pump pulse which is up-chirped meanwhile, and the gain profile follows a Lorentzian function with a half-width-half-maximum (HWHM) linewidth of Γ, as shown in Fig.1 (a). When the central frequency of the pump pulse locates at $\nu_s + \nu_1$, which is red-detuned from the peak gain position at $\nu_s + \nu_R$, its trailing edge will be less shifted from the Raman peak compared with its leading edge, as shown in the left graph in Fig.1 (b). There is a time point t_1 in the trailing edge, at which the frequency of that part of the pulse is exactly matched to the Raman resonance, i.e., $\Delta\nu = 0$, as depicted in the left graph of Fig. 1(c). Then instead of at the pump peak, the maximum Raman amplification happens at its

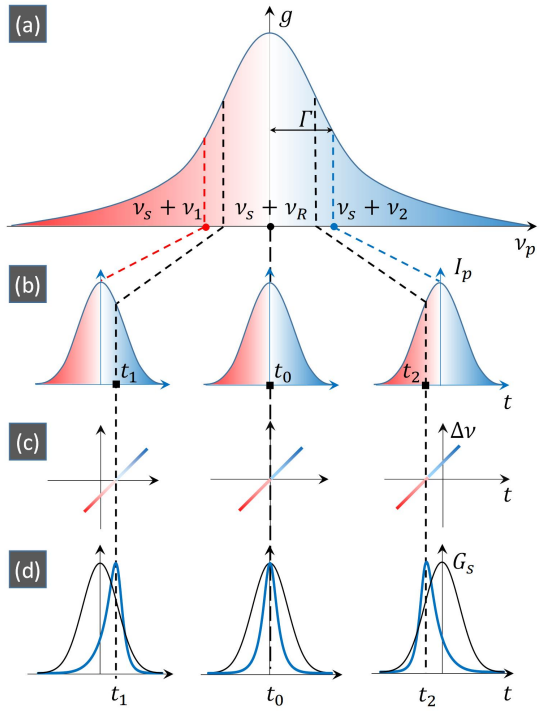

Fig. 1 Illustration of time-shift of signal pulse center induced by a frequency-chirped pump pulse. (a) A typical Raman gain profile in Lorentzian shape, where ν_s, ν_p and ν_R are the optical frequency of signal beam, pump beam and Raman resonance respectively, g is Raman gain factor; (b) Linearly up–chirped pump pulse with central frequency red-, zero- and blue-detuned from Raman resonance; (c) Instantaneous frequency detuning for time points within pump; (d) The resulting time-dependent signal gain. The gradient color from red to blue represents the degree of frequency detuning; The red and blue dashed line indicates the central frequency of pump pulse; The black dashed line indicates the point of zero-detuning in pump pulse.

trailing edge around t_1. So the gravity center of the generated signal pulse lags behind the pump, shown as the blue line in the left graph of Fig. 1(d), where, for comparison, the black line is the signal pulse excited by the same pump pulse without frequency chirp. On the other hand, if the central frequency of pump pulse is blue detuned to $\nu_s+\nu_2$, the zero-detuning point appears in the leading edge at t_2, depicted as the right graphs in Fig. 1(a-c). Then the gravity center of the generated signal pulse moves forward in time, shown as the blue line in the right graph of Fig. 1(d). If there is no detuning for the central wavelength of pump pulse, there will be no shift in time for the signal with its peak synchronized to the pump peak at t_0, shown as the mid graphs in Fig. 1(a-d). It is also found that the width of signal pulses excited by the frequency-chirped pump are narrower in time than those without chirp in all of the three cases, as shown in Fig. 1(d). This is caused by the nonzero slope of the detuning vs. time curve in Fig. 1(c), which results in fast drop of gain coefficient G_s within the pulse. For simplicity, we may just suppose the Raman amplification process to be a steady-state case, which, however, is strictly satisfied only when the pulse width far exceeds Γ^{-1} [14]. Then the time-dependent gain for signal beam could be expressed as:

$$G_s(t) \sim \frac{g_0 I_p L \Gamma^2}{[\Delta\nu_0+\nu_c(t)]^2+\Gamma^2} e^{-4\ln 2(t/\tau)^2}. \quad (1)$$

where, g_0 is the on-resonance gain factor, I_p is peak intensity of pump, L is optical path, $\Delta\nu_0 = \nu_{p0} - (\nu_s+\nu_R)$ is the detuning of pump center ν_{p0} with respect to Raman resonance at $\nu_s+\nu_R$, τ is full-width-half-maximum (FWHM) pulse width of pump, and $\nu_c(t)$ is the time-dependent frequency chirp for pump pulse.

The experiment of tunable delay of signal peak is based on SRG in hydrogen through the evanescent field of an optical NF. The intensive evanescent field associated with the NF greatly enhances the SRG efficiency. Although the higher Raman efficiency does not necessarily result in larger shift range, which is only determined by the frequency chirping amplitude in this experiment, it does enhance the signal amplitude for a fixed pump power. The 4.8-cm-long and 700-nm-diameter NF has a total transmission of 60 % and is sealed in an aluminum gas cell with two SMF pigtails left outside for optical connection. Pure hydrogen is filled and works as the Raman gain medium through the evanescent field of NF. As shown in Fig. 2, the pump beam is from a DFB laser with its center wavelength tuned around 1532.831 nm using a temperature controller. The AOM is driven by a pulse generator with rate of 200 kHz. The modulated pump is injected into an EDFA and amplified to a near-Gaussian shaped pulse with peak power of 18 W and FWHM width of 17 ns, as measured before entering the WDM. The seeded cw signal beam is from the ECDL with a fixed wavelength of 1620.876 nm. The frequency difference between the pump and signal is about 10.624 THz, matching the $S_0(0)$ Raman transition of hydrogen. For the case of 700-nm-diameter NF, the HWHM linewidth of the hydrogen at atmospheric pressure is measured to be $\Gamma = 119\ MHz$, which is about two times of the free space case. This broader linewidth is attributed to the additional transit-time broadening, due to the small evanescent field area of NF and fast molecular velocity of hydrogen [15]. The shape of the amplified signal beam with respect to pump detuning is monitored by an oscilloscope. The frequency chirp for pump pulse is introduced by SPM along with pulse amplification and propagation in EDFA and fiber transmission line. The chirping amplitude can be adjusted by splicing a section of standard single mode fiber (SMF) between points A and B, according to $\nu_c(t) = -n_2 L \lambda^{-1} I'(t)$ [16]. When

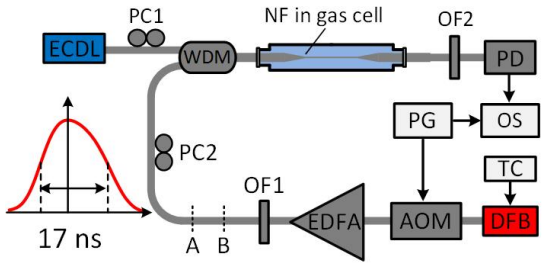

Fig. 2 Experimental setup for observing tunable delay of signal peak. DFB: distributed feedback laser; TC: temperature controller; AOM: acousto-optic modulator; EDFA: erbium doped fiber amplifier; OF1: optical filter 1, centers at 1532.8 nm to eliminate ASE noise from EDFA; PC: polarization controller; ECDL: external cavity diode laser; WDM: wavelength division multiplexer; OF2: optical filter 2, centers at 1620.9 nm for elimination of the pump beam; PD: photodetector; OS: oscilloscope; PG: pulse generator. Inset: measured shape of pump pulse before its entering into the WDM.

there is no additional piece of SMF inserted, the frequency chirping amplitude of the pump pulse is measured to be 37 MHz before entering the nanofiber. The effect of SPM in the nanofiber and its transition region are neglected due to their relatively short length.

Shown in Fig. 3(a) are the normalized signal pulse shapes along with center wavelength sweeping of the pump beam in the range corresponding to Raman detuning ν_d from -80 to 80 MHz. When the pump goes from red- to blue-detuned, the Raman-generated signal pulse moves forward in time, resulting in a change from delay of 2.3 ns to advancement of 2.3 ns for its peak. The SRS gain and peak position for the signal pulse along with pump wavelength sweeping across the whole $S_0(0)$ Raman line are shown in Fig. 3(b). Compared with delay of pulse peak, the magnitude of advancement is about one nanosecond larger. This is caused by the asymmetric shape of pump pulse, as shown in the inset of Fig. 2. The leading edge of pump pulse is a bit steeper than the trailing one, which results in more negative frequency shift in the leading edge than the positive shift in the trailing edge. Compared with the simulated curve (blue solid line), which is obtained from Equ. (1) based on the experimentally measured shape and chirping amplitude of pump pulse, there is an ~0.5 ns delay at resonance, as shown in the inset of Fig. 3(b). This delay is due to the transient effect in SRS that the build-up of material excitation tends to increase the gain for the next moment and thus push the signal peak backwards in time. Shown in Fig. 3(c) is the simulation results for a cw signal being Raman-amplified by a pump pulse with fixed pulse width of τ, according to the theory given by Carman [17]. With reduced time-linewidth product $\tau\Gamma$, the gravity center of generated signal pulse gradually shifts backward and so does the signal peak, as depicted by the red dashed line. The experiment here is closer to the case of $\tau\Gamma = 3$ shown as the orange solid line, which indicates a peak delay of 0.05τ at Raman resonance, i.e, 0.85 ns. A short of 0.35 ns here may result from the frequency chirp in our case, which is not covered by the theory as well as in the simulation. The minimum width of the generated signal pulses is about 13.5 ns, which is 20 % less than the pump's. The narrower pulse width originates from the additional gain reduction within the time span of pump pulse except at the zero-detuning position, as indicated in Fig. 1(d). It should also be mentioned that the spectrum-independent Raman signal from the silica, which has a magnitude about one tenth of the hydrogen peak, has been subtracted from the gain spectrum in Fig. 3(b). The Raman gain signal from hydrogen is relatively small here, with its peak power about 25 times less than the seeded background. It is easier to demonstrate the tunable shift of signal peak in a cw beam, compared to a pulsed beam, which requires a gain at least one order of magnitude larger than the current level.

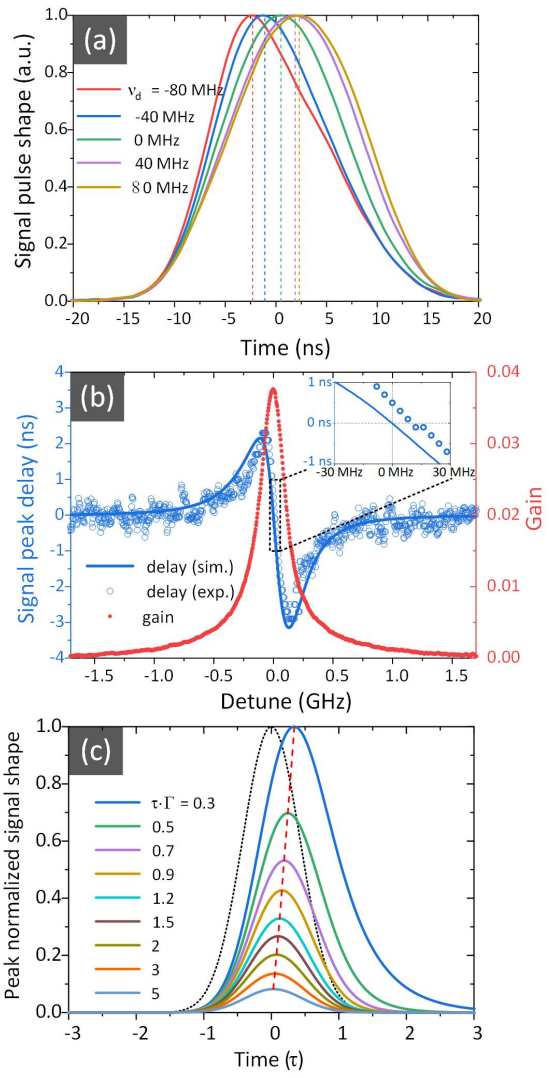

Fig. 3 (a) Experimentally measured signal pulse shape with Raman detuning from -80 to 80 MHz. The dashed lines indicate the positions of signal peak. (b) Measured peak position (blue circles) and SRS gain (red dots) for the signal pulses with Raman detuning from -1.7 to 1.7 GHz. The blue line is the simulated curve of delay vs detuning. (c) Simulation results of transient Raman effect. The black dotted line represents the shape of pump pulse with fixed pulse width of τ. The red dashed line indicates the peak position of generated signal pulse.

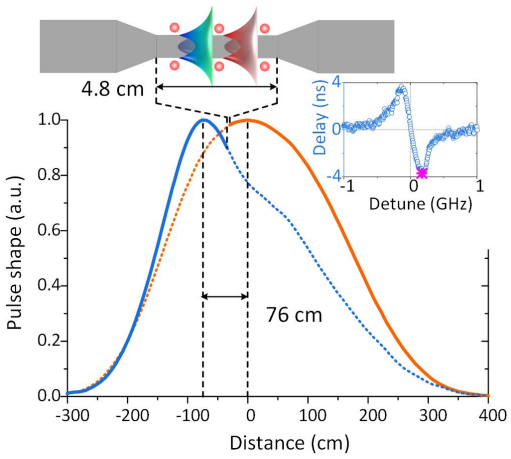

Fig. 4 A snap shot of positions of signal and pump pulses. The blue solid and orange dotted lines represent the parts of signal and pump having left the NF, while the blue dotted and orange solid lines represent the parts of signal and pump will enter into the NF. The reddish balls surrounding the nanofiber represents hydrogen molecules.

As the amplitude of frequency chirp is less than the linewidth of Raman transition here, larger tuning range can be realized by increasing the chirping amplitude. This is achieved by introducing an additional section of 75 m SMF between points A and B in Fig. 2, which increases the magnitude of SPM induced frequency chirp to 63 MHz for the same pump pulse. Tunable delay of signal peak ranging from -3.7 to 3.7 ns is achieved by pump frequency tuning of less than 400 MHz, shown as the inset of Fig. 4. Due to the increased magnitude of frequency chirp, the minimum signal pulse width is reduced to ~12 ns. An advanced signal pulse, indicated as the asterisk marker in the inset, propagating through the taper is shown as the blue line (both solid and dashed) in Fig. 4. It can be found that the signal peak has already left the NF before the pump peak entering into it. A total lead of 76 cm for the signal peak over the pump's is achieved for a 170 MHz blue-detuning of the pump center off the Raman resonance.

The delay tuning is also determined by the linewidth of Raman gain profile. A bonus for working with gas phase SRG medium is the convenience of adjusting the linewidth by pressure. As an example, by increasing the hydrogen pressure from 1 to 2 bar, the linewidth is increased by 8 % and the delay tuning range is reduced by 7 %, although the gain is increased by about 80 %. The reduction of tuning range here is due to the relatively small magnitude of frequency chirping compared with the linewidth of Raman transition. The shape and position of the generated signal pulse can also be controlled by the frequency chirping function, as illustrated by the numerical results in Fig. 5. The Gaussian-shaped pump pulse has a HWHM pulse width of Γ^{-1}, where Γ is the HWHM linewidth of the Raman line. The pump pulses are frequency chirped in linear, tangent, arctangent and cubic functions respectively, and have the same chirping amplitude of 2Γ, within the time span of $\pm 3\Gamma^{-1}$. The red, blue and purple solid lines are the time-dependent gain for the signal beam when the pump is $-\Gamma$, 0 and Γ detuned from the Raman resonance. The results are obtained from Equ. (1), without consideration of transient effect in SRG, which cannot be neglected when the pump width is considerably shorter than Γ^{-1}.

To summarize, we report a novel technique of all-optical delay tuning for signal beam by frequency chirped pump pulse in SRG.

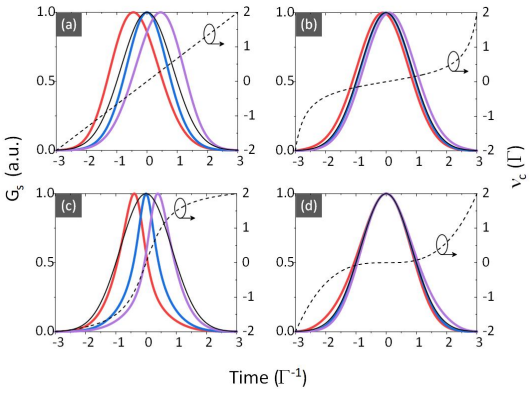

Fig. 5 Simulated time dependent signal gain coefficient by pulsed pump with (a) linear, (b) tangent, (c) arctangent and (d) cubic frequency chirping functions. The black solid lines are the gain without frequency chirp, the dashed lines represents instantaneous chirping value ν_c.

The tunable delay of signal peak comes from the controllable position of maximum Raman gain within the span of a frequency chirped pump pulse. Continuous adjustment of 0.6 fractional delay of signal peak is achieved experimentally based on SRS in hydrogen. The delay tuning range is generally limited within one pulse width, which is relatively low compared with techniques based on SBS or DDL. So, for the potential application in optical signal processing, this technique may work as a complementary method for these large-buffering-capacity techniques, to precisely adjust the signal peak within one-bit time. Considering the pulse shaping ability of this technique, it may also be used for restoration of distorted signal with properly designed chirping function for pump pulse. An advantage inherent in gas-phase Raman medium is the convenience of switching to different molecular species as well as their different Raman transition lines, which makes it highly flexible in choosing operation wavelength compared with EIT or CPO, where the transition lines are fixed. In addition, by changing the gas pressure, the linewidth of the gain profile can be readily increased up to tens of GHz, meeting the needs for tunable delay of ps pulses.

Funding. The National Key Research and Development Program of China (2019YFB2203904), Hong Kong Special Administrative Region Government (15260316), National Natural Science Foundation of China (61827820, 61535004), The Local Innovative and Research Teams Project of Guangdong Pear River Talents Program (2019BT02X105), The Hong Kong Polytechnic University (1-9B65).

Disclosures. The authors declare no conflicts of interest.

References

1. A. E. Willner, B. Zhang, L. Zhang, L. Yan, and I. Fazal, IEEE Journal of selected topics in quantum electronics **14**, 691-705 (2008).
2. R. W. Boyd, and D. J. Gauthier, Science **326**, 1074-1077 (2009).
3. L. V. Hau, S. E. Harris, Z. Dutton, and C. H. Behroozi, Nature **397**, 594 (1999).
4. L. J. Wang, A. Kuzmich, and A. Dogariu, Nature **406**, 277-279 (2000).
5. M. S. Bigelow, N. N. Lepeshkin, and R. W. Boyd, Physical review letters **90**, 113903 (2003).
6. Y. Okawachi, M. S. Bigelow, J. E. Sharping, Z. Zhu, A. Schweinsberg, D. J. Gauthier, R. W. Boyd, and A. L. Gaeta, Physical review letters **94**, 153902 (2005).
7. K. Y. Song, M. G. Herráez, and L. Thévenaz, Opt. Express **13**, 82-88 (2005).
8. L. Thévenaz, Nature photonics **2**, 474 (2008).
9. R. Pant, A. Byrnes, C. G. Poulton, E. Li, D.-Y. Choi, S. Madden, B. Luther-Davies, and B. J. Eggleton, Opt. Lett. **37**, 969-971 (2012).
10. J. E. Sharping, Y. Okawachi, and A. L. Gaeta, Opt. Express **13**, 6092-6098 (2005).
11. Y. Okawachi, M. A. Foster, J. E. Sharping, A. L. Gaeta, Q. Xu, and M. Lipson, Opt. Express **14**, 2317-2322 (2006).
12. J. E. Sharping, Y. Okawachi, J. van Howe, C. Xu, Y. Wang, A. E. Willner, and A. L. Gaeta, Opt. Express **13**, 7872-7877 (2005).
13. Z. Shi, A. Schweinsberg, J. E. Vornehm Jr, M. A. M. Gámez, and R. W. J. P. L. A. Boyd, **374**, 4071-4074 (2010).
14. M. Maier, and G. Renner, Optics Communications **3**, 301-304 (1971).
15. Y. Qi, W. Jin, and H. L. Ho, Opt. Express **28**, 8324-8330 (2020).
16. G. P. Agrawal, "Nonlinear fiber optics," in *Nonlinear science at the dawn of the 21st century*(Springer, 2000), pp. 195-211.
17. R. L. Carman, F. Shimizu, C. Wang, and N. Bloembergen, Physical Review A **2**, 60 (1970).